

## ORIGINAL ARTICLE

# Antibacterial activity of biogenic silver nanoparticles synthesized with gum ghatti and gum olibanum: a comparative study

Aruna Jyothi Kora<sup>1</sup> and Rao Beedu Sashidhar<sup>2</sup>

Presently, silver nanoparticles produced by biological methods have received considerable significance owing to the natural abundance of renewable, cost-effective and biodegradable materials, thus implementing the green chemistry principles. Compared with the nanoparticles synthesized using chemical methods, most biogenic silver nanoparticles are protein capped, which imparts stability and biocompatibility, and enhanced antibacterial activity. In this study, we compared the antibacterial effect of two biogenic silver nanoparticles produced with natural plant gums: gum ghatti and gum olibanum against Gram-negative and Gram-positive bacteria. Bacterial interaction with nanoparticles was probed both in planktonic and biofilm modes of growth; employing solid agar and liquid broth assays for inhibition zone, antibiofilm activity, inhibition of growth kinetics, leakage of intracellular contents, membrane permeabilization and reactive oxygen species production. In addition, cytotoxicity of the biogenic nanoparticles was evaluated in HeLa cells, a human carcinoma cell line. Antibacterial activity and cytotoxicity of the silver nanoparticles synthesized with gum ghatti (Ag NP-GT) was greater than that produced with gum olibanum (Ag NP-OB). This could be attributed to the smaller size (5.7 nm), monodispersity and zeta potential of the Ag NP-GT. The study suggests that Ag NP-GT can be employed as a cytotoxic bactericidal agent, whereas Ag NP-OB (7.5 nm) as a biocompatible bactericidal agent.

*The Journal of Antibiotics* (2015) 68, 88–97; doi:10.1038/ja.2014.114; published online 20 August 2014

## INTRODUCTION

Most of the chemical methods used for metallic nanoparticle synthesis require toxic organic solvents and reactive reducing agents, which pose environmental and biological risks.<sup>1,2</sup> Conversely, physical methods necessitate sophisticated equipment, stringent conditions, are limited to low production rates, high energy consumption and consequently high cost.<sup>3</sup> Thus, the thrust has shifted toward green chemistry-based synthesis of nanoparticles using biologicals, as a simple and viable alternative. Furthermore, there is natural abundance of renewable, cost-effective and biodegradable materials from diverse sources including bacteria,<sup>4</sup> fungi,<sup>5</sup> algae<sup>6</sup> and plants.<sup>7</sup> Most of the chemogenic silver nanoparticles are cytotoxic and nonbiocompatible due to contamination from chemical precursors, residual solvent toxicity and generation of hazardous by-products and so on.<sup>8</sup> Hence, they are not ideal candidates for biomedical or pharmaceutical applications. In this context, we have explored and developed facile and green routes for the synthesis of silver nanoparticles from silver nitrate using nontoxic, renewable natural plant polymers of Indian origin: gum ghatti (*Anogeissus latifolia*)<sup>9</sup> and gum olibanum (*Boswellia serrata*).<sup>10</sup>

Toxicity of silver nanoparticles synthesized by various reductants and methodologies has been demonstrated to a number of bacteria

including *Escherichia coli*, *Pseudomonas aeruginosa*, *Staphylococcus aureus*, methicillin-resistant *S. aureus*, *S. epidermidis*, *Streptococcus faecalis*, *Bacillus subtilis*, *Mycobacterium smegmatis*, *M. bovis*, *Vibrio cholera*, *Salmonella typhus*, *Enterococcus faecalis*, *E. faecium*, *Klebsiella pneumoniae*, *Syphilis typhus* and *Acinetobacter baumannii*.<sup>11–15</sup> A recent comparative study of biogenic and protein-capped silver nanoparticles and chemically synthesized silver nanoparticles found that, biogenic nanoparticles were more bactericidal than chemically synthesized nanoparticles.<sup>16</sup> The present study compares the antibacterial activity of two biogenic, protein-capped silver nanoparticles synthesized from two natural plant gums against Gram-negative and Gram-positive planktonic and biofilm bacteria. The integrated methodologies used include well diffusion, micro-broth dilution, antibiofilm activity, bacterial growth kinetics, leakage of cytoplasmic contents and membrane permeabilization assay, and impact of reactive oxygen species (ROS) on antibacterial activity.

## MATERIALS AND METHODS

### Bacterial strains and silver nanoparticles

Gram-negative (*E. coli* ATCC 25922, *E. coli* ATCC 35218, *P. aeruginosa* ATCC 27853) and Gram-positive (*S. aureus* ATCC 25923) bacteria were used as model test strains. The methods for silver nanoparticle preparation using gum

<sup>1</sup>National Centre for Compositional Characterisation of Materials (NCCCM), Bhabha Atomic Research Centre, Hyderabad, India and <sup>2</sup>Department of Biochemistry, University College of Science, Osmania University, Hyderabad, India  
Correspondence: Professor RB Sashidhar, Department of Biochemistry, University College of Science, Osmania University, Hyderabad, Andhra Pradesh 500 007, India.  
E-mail: sashi\_rao@yahoo.com

Received 7 May 2014; revised 30 June 2014; accepted 13 July 2014; published online 20 August 2014

ghatti and gum olibanum were standardized using methods previously reported.<sup>9,10</sup> In brief, gum ghatti silver nanoparticles (Ag NP-GT) with a mean particle size of  $5.7 \pm 0.2$  nm were synthesized by autoclaving 0.1% gum ghatti solution containing 1 mM silver nitrate at 121 °C, 15 psi for 30 min. Gum olibanum silver nanoparticles (Ag NP-OB) with a mean particle size of  $7.5 \pm 3.8$  nm were prepared by autoclaving 0.5% gum olibanum extract containing 1 mM silver nitrate at 121 °C, 15 psi for 30 min (Supplementary Figure 1). The inductively coupled plasma-optical emission spectrometer (ICP-OES) technique was employed to determine the total silver content in the synthesized nanoparticles. The samples were digested with ultra-pure nitric acid and the digested samples were analyzed using a Jobin Yvon Horiba JY-2000 ICP-OES (Longjumeau, France) equipped with a Meinhard concentric nebulizer and a cyclonic spray chamber. The zeta potential of the nanoparticle solutions was measured with a Malvern Zetasizer Nanosystem (Malvern, UK). The absorbance and fluorescence measurements were carried out with Biotek Synergy H1 plate reader (Winooski, VT, USA).

### Antibacterial assays

**Well diffusion assay.** The bacterial suspension was prepared by growing a single colony overnight in nutrient broth and adjusting the turbidity to 0.5 McFarland standard. Mueller Hinton agar (MHA) plates were inoculated with this bacterial suspension and 5 µg of silver nanoparticles were added to the center well with a diameter of 6 mm. The negative control plates were maintained with autoclaved gum-loaded wells. Erythromycin (15 µg per disk) (HiMedia Chemicals Pvt. Ltd, Mumbai, India)-loaded culture plates were included as positive control. Plates were incubated at 37 °C for 24 h in a bacteriological incubator and the zone of inhibition (ZOI) was calculated as  $ZOI = \text{diameter of total inhibition} - \text{diameter of the well}$ .

**Micro-broth dilution method.** The micro-broth dilution method<sup>17</sup> was used to determine the MIC and MBC of silver nanoparticles against test bacterial strains. Sterile polystyrene microtiter plate wells were inoculated with 200 µl of nutrient broth containing  $10^6$  CFU ml<sup>-1</sup> and loaded with different concentrations of nanoparticles (1–15 µg ml<sup>-1</sup>). Plates were incubated in static mode at 37 °C for 48 h. Control wells were maintained with medium containing bacterial suspension. Bacterial growth was measured by visual inspection for turbidity, and absorbance at 600 nm. The concentration at which there was no increase in absorbance was taken as the MIC. A volume of 100 µl of bacterial suspension from each negative well (no visual turbidity) was plated on nutrient agar. The lowest concentration at which no colonies formed on nutrient agar plates was taken as the MBC.

**In vitro biofilm formation assay.** The effect of silver nanoparticles on biofilm formation was assessed by a modified microtiter plate assay.<sup>18</sup> Sterile polystyrene microtiter plate wells were inoculated with 200 µl of nutrient broth containing  $10^6$  CFU ml<sup>-1</sup> and loaded with 2 µg ml<sup>-1</sup> of silver nanoparticles. The plates were incubated in static mode at 37 °C for 48 h. The negative and positive control wells were maintained without silver nanoparticles and ciprofloxacin-treated bacterial suspensions, respectively. After 48 h of growth, the medium in the wells was removed and washed with sterile PBS to remove loosely attached bacteria. Wells were then stained with 200 µl of 0.1% crystal violet and incubated for 30 min, washed and air dried. Bound stain was solubilized in 200 µl of 95% ethanol, and absorbance measured at 590 nm.

**Bacterial growth curve.** The bacterial growth curve was monitored by inoculating the microtiter plate wells with nutrient broth containing  $10^6$  CFU ml<sup>-1</sup> and loaded with various concentrations of nanoparticles (1–10 µg ml<sup>-1</sup>). The plates were incubated at 37 °C, 100 r.p.m. and the absorbance was recorded at 600 nm for 48 h using Biotek Synergy H1 plate reader.<sup>15</sup>

**Leakage of cytoplasmic contents.** The effect of silver nanoparticles on membrane damage was studied by quantifying leaked cytoplasmic nucleic acids and proteins.<sup>19–21</sup> The bacterial cell suspension with an absorbance 0.5 at 600 nm was prepared in sterile saline and treated with 5 µg ml<sup>-1</sup> of silver nanoparticles for 1 h. The negative and positive controls were maintained

without silver nanoparticles and by boiling the suspensions at 100 °C for 30 min. Samples were centrifuged at 10 000 r.p.m. for 10 min and supernatants were measured for absorbance at 260 and 280 nm.

**Outer membrane damage.** The outer membrane damage in Gram-negative bacteria induced by silver nanoparticles was monitored using a fluorescent probe, *N*-phenyl naphthylamine (NPN) permeabilization assay.<sup>20,22</sup> A stock solution of 5 mM NPN in acetone was diluted with 5 mM HEPES buffer, pH 7.2 to make a 0.2 mM NPN working solution. Gram-negative *P. aeruginosa* 27853, *E. coli* 25922 and *E. coli* 35218 were used in the assay. Bacterial cultures in nutrient broth were grown overnight, harvested, washed and resuspended in 5 mM HEPES buffer, pH 7.2 and the suspension was adjusted to obtain an absorbance 0.5 at 600 nm. Silver nanoparticles (3 µg ml<sup>-1</sup>) were added to 10 µl of 0.2 mM NPN solution in black microtiter plates. A volume of 200 µl bacterial suspension was added to the above mixture and incubated at 37 °C for 10 min. Bacterial suspensions without silver nanoparticles and with 30 µM H<sub>2</sub>O<sub>2</sub> served as negative and positive controls, respectively. Fluorescence at 420 nm with an excitation wavelength of 350 nm was recorded.

**Effect of antioxidant on bactericidal activity of silver nanoparticles.** To assess the impact of free radicals on the bactericidal activity of silver nanoparticles, MHA plates were supplemented with silver nanoparticles at 5 µg ml<sup>-1</sup>. The antioxidant *N*-acetylcysteine (NAC) was added to these plates at 10 mM concentration. These plates were inoculated with known CFU of bacteria by spread plating and the number of surviving bacteria was counted after 24 h of incubation at 37 °C. The nanosilver-free control plates were maintained with NAC.<sup>12</sup>

**Detection of intracellular ROS.** The generation of intracellular ROS generation in nanoparticle-treated bacterial cells was determined using dichlorodihydrofluorescein diacetate (H<sub>2</sub>DCFDA), an intracellular ROS indicator. A stock solution of 2 mM H<sub>2</sub>DCFDA was prepared in dimethyl sulfoxide and stored under dark at -40 °C. The overnight grown bacterial cultures in nutrient broth were harvested, washed and resuspended in 0.1 M sodium phosphate buffer, pH 7.2 and the cell suspension was adjusted to obtain an A<sub>600 nm</sub> of 0.5. To 20 ml of the bacterial suspension, 100 µl of 2 mM H<sub>2</sub>DCFDA stock solution was added to get a final concentration of 10 µM and incubated under dark at 37 °C for 60 min. After washing, the cells were suspended in the same buffer and the 200 µl of H<sub>2</sub>DCFDA-treated, washed bacterial cell suspensions were aliquoted in a 96-well black plate and 2 µg ml<sup>-1</sup> of silver nanoparticles were added and incubated under dark at 37 °C. The negative and positive controls were maintained with nanosilver-free and 30 µM H<sub>2</sub>O<sub>2</sub>-treated bacterial suspensions, respectively. After 60 min of incubation, the fluorescence intensity was recorded at an excitation wavelength of 490 nm and an emission wavelength of 520 nm.<sup>11</sup>

**MTT assay.** For evaluating the cytotoxicity of the prepared nanoparticles on mammalian cells, the 3-(4, 5 dimethyl-2-yl)-2, 5-diphenyltetrazolium bromide (MTT) assay<sup>23</sup> was carried out with human cervical cancer cell line HeLa. The 96-well microtiter plates were seeded with  $10^5$  cells per well in Dulbecco's modified Eagle's medium containing 10% serum at 5% CO<sub>2</sub> concentration and exposed to silver nanoparticles at different concentrations (1, 2.5, 5, 10, 25 and 50 µg ml<sup>-1</sup>) and incubated for 24–72 h at 37 °C in a INC 108 Memmert CO<sub>2</sub> incubator (Memmert, Schwabach, Germany). The negative and positive controls were maintained with nanosilver-free and doxorubicin (13 µg ml<sup>-1</sup>)-treated cells, respectively. After the completion of exposure, the medium was removed from each well and was replaced with 200 µl of fresh medium containing 10 µl of MTT (5 mg ml<sup>-1</sup>) and incubated for 4 h at 37 °C. The medium was decanted and the resulting formazan crystals were dissolved in 200 µl of dimethyl sulfoxide per well. The absorbance was measured at 540 nm using Biotek Synergy H1 plate reader and the % viability was calculated by considering untreated controls as 100% viable.

## RESULTS AND DISCUSSION

### Zone of inhibition

The well diffusion method was used to study the antibacterial activity of the synthesized silver nanoparticles. After 24 h of incubation at 37 °C, growth suppression was observed in plates loaded with 5 µg of

silver nanoparticles and negative control plates loaded with either of the autoclaved gum did not produce any ZOI. As expected, the positive control plates loaded with erythromycin antibiotic exhibited considerable inhibition zones. The ZOI observed with both the silver nanoparticles against various bacterial strains are shown in Table 1. The ZOI recorded with all test strains was in the order of Ag NP-GT > Ag NP-OB. It was earlier reported that the antibacterial activity of the nanoparticles is directly proportional to the zeta potential.<sup>24</sup> The measured zeta potential values for the Ag NP-GT and Ag NP-OB were  $-22.4 \pm 8.7$  mV and  $-14.9 \pm 6.6$  mV, respectively.

In a strain-specific antibacterial study, ZOI of 14–15 and 16 mm were reported for *S. aureus* and *E. coli* strains, respectively. These thiol-capped nanoparticles with an average size of 3.3 nm were produced by borohydride reduction and used at a nanosilver loading of 100  $\mu\text{g}$ . Thus, the effective inhibition observed in our studies was found to be higher than the reported values for chemically produced silver nanoparticles.<sup>25</sup> To further evaluate the results, we have compared our data with the available reports on biogenic silver nanoparticles. With the same strains, ZOI of 9 and 8 mm were noted at 20  $\mu\text{g}$  loading. Here, the silver nanoparticles of 3–30 nm size were biosynthesized by the fungus *Aspergillus niger*.<sup>26</sup> Thus, the ZOI values observed by us with silver nanoparticles synthesized by gums at 5  $\mu\text{g}$  loading were higher than the reported values. On the basis of these results, it can be concluded that both the biogenic nanoparticles had significant antibacterial action on both the Gram classes of bacteria. In addition to particle size, the surface-capping agent has an important role in determining the bactericidal activity of silver nanoparticles.<sup>16,27</sup> Hence, the biogenic antibacterial silver nanoparticles generated with gums have advantage over other chemically produced (chemogenic) nanoparticles.

#### Determination of MIC and MBC

The growth inhibition effect of silver nanoparticles against bacterial strains was measured by MIC. For *S. aureus* 25923, *P. aeruginosa* 27853, *E. coli* 25922 and *E. coli* 35218, the MIC values of both the silver nanoparticles were 10.0, 5.0, 2.0 and 2.0  $\mu\text{g ml}^{-1}$ , respectively. In a previous antibacterial study, MIC values of 8–32, 16 and 32  $\mu\text{g ml}^{-1}$  were reported for *S. aureus*, *P. aeruginosa* and *E. coli* strains, respectively. These nanoparticles of 13 nm size were prepared using culture supernatant of *P. aeruginosa*.<sup>4</sup> For the respective *S. aureus*, *P. aeruginosa* and *E. coli* strains, the MIC values were observed to be lower by 3.2-, 3.2- and 16-fold, respectively. Thus, the silver nanoparticles synthesized using plant gums were found to be more potent bactericidal agents in terms of concentration. The highest value of MIC was noted for *S. aureus* 25923 followed

by *P. aeruginosa* 27853. The lowest value of MIC was observed for both the *E. coli* strains. From the results, it is evident that among the strains selected for testing, *E. coli* was more sensitive toward the bactericidal activity of silver nanoparticles used in this study. These findings on susceptibility of *E. coli* toward silver nanoparticles are in line with the earlier-reported studies.<sup>11,12</sup>

Most of the MBC values were same as MIC and with *P. aeruginosa* 27853 a MBC value of 12  $\mu\text{g ml}^{-1}$  was noted for both the nanoparticles. Also, higher MBC values were observed for *S. aureus* 25923 (12  $\mu\text{g ml}^{-1}$ ) and *E. coli* 35218 (3  $\mu\text{g ml}^{-1}$ ) with Ag NP-OB. The MBC values detected for *S. aureus* and *E. coli* strains were lower by 4 and 33 $\times$ , respectively; when compared with PVP-stabilized nanoparticles of 10 nm size synthesized by ultrasonic irradiation.<sup>11</sup>

#### Antibiofilm activity

The inhibition of biofilm formation by silver nanoparticles was studied with static microtiter plate assay at a concentration of 2  $\mu\text{g ml}^{-1}$  (Table 2). The Ag NP-GT was able to impede the biofilm formation by 92.9%, 81.1%, 78.7% and 64.5%, respectively in *E. coli* 35218, *E. coli* 25922, *P. aeruginosa* 27853 and *S. aureus* 25923. Against the same strains, inhibition was 92.9%, 82.9%, 77.0% and 61.4% with Ag NP-OB, respectively. In the case of positive control, the observed inhibition was 93.3%, 83.1%, 39.4% and 73.4% with the respective bacterial strains. Notably, the activity of both the biogenic nanoparticles against *P. aeruginosa* 27853 biofilm formation was nearly twofold as compared with the positive control ciprofloxacin. The employed silver particles exhibited more or less similar antibiofilm activity against the rest of the test strains. Among the selected strains, *S. aureus* 25923 and *P. aeruginosa* 27853 were least susceptible to the antibiofilm activity of nanoparticles owing to the production of exopolysaccharides, which are needed for bacterial adhesion to the surface during biofilm formation.<sup>28</sup> These results indicate that the biogenic silver nanoparticles synthesized with plant gums demonstrate strong bactericidal activity as well as antibiofilm activity.

#### Bacterial growth kinetics in the presence of nanosilver

The growth inhibition of bacteria was investigated in nutrient broth supplemented with silver nanoparticles (0–10  $\mu\text{g ml}^{-1}$ ) for 48 h at 600 nm. The kinetics of all the growth curves obey typical pattern; a lag phase, an exponential phase and a stationary phase. For *E. coli* 25922, the lag phase was reduced to 3 h for the concentrations up to 5  $\mu\text{g ml}^{-1}$  of Ag NP-GT. Even the highest tested concentrations of 10  $\mu\text{g ml}^{-1}$  limited the lag phase to 4 h and did not cause complete growth inhibition (Figure 1a). In the case of Ag NP-OB, the concentrations beyond 4  $\mu\text{g ml}^{-1}$  induced a lag phase for 8 h and

**Table 1** The inhibition zones (mm) observed with different bacterial culture plates loaded with biogenic silver nanoparticles and erythromycin

| Test compound ( $\mu\text{g}$ ) | Zone of inhibition (mm) <sup>a</sup> |                            |                      |                      |
|---------------------------------|--------------------------------------|----------------------------|----------------------|----------------------|
|                                 | <i>S. aureus</i> 25923               | <i>P. aeruginosa</i> 27853 | <i>E. coli</i> 25922 | <i>E. coli</i> 35218 |
| Ag NP-GT (5)                    | 12.2 $\pm$ 0.2                       | 11.0                       | 9.0                  | 8.0 $\pm$ 0.1        |
| Ag NP-OB (5)                    | 10.7 $\pm$ 0.2                       | 7.5                        | 8.0 $\pm$ 1.0        | 5.5                  |
| Erythromycin (15)               | 23.5 $\pm$ 1.0                       | 11.0 $\pm$ 1.1             | 7.0 $\pm$ 1.1        | 9.0 $\pm$ 1.1        |

Abbreviations: Ag NP-GT, silver nanoparticles synthesized with gum ghatti; Ag NP-OB, silver nanoparticles synthesized with gum olibanum.

<sup>a</sup>Values are mean  $\pm$  s.d. ( $n=3$ ).

**Table 2** The percentage inhibition in biofilm formation by different bacterial strains treated with biogenic silver nanoparticles and ciprofloxacin

| Test compound ( $\mu\text{g ml}^{-1}$ ) | Biofilm inhibition (%) <sup>a</sup> |                            |                      |                      |
|---|-------------------------------------|----------------------------|----------------------|----------------------|
|   | <i>S. aureus</i> 25923              | <i>P. aeruginosa</i> 27853 | <i>E. coli</i> 25922 | <i>E. coli</i> 35218 |
| Ag NP-GT (2)                            | 64.5 $\pm$ 3.5                      | 78.7 $\pm$ 0.8             | 81.1 $\pm$ 1.5       | 92.9 $\pm$ 0.4       |
| Ag NP-OB (2)                            | 61.4                                | 77.0 $\pm$ 1.6             | 82.9 $\pm$ 0.4       | 92.9 $\pm$ 0.4       |
| Ciprofloxacin (0.1)                     | 73.0                                | 39.4 $\pm$ 3.5             | 83.1                 | 93.3 $\pm$ 0.6       |

Abbreviations: Ag NP-GT, silver nanoparticles synthesized with gum ghatti; Ag NP-OB, silver nanoparticles synthesized with gum olibanum.

<sup>a</sup>Values are mean  $\pm$  s.d. ( $n=3$ ).

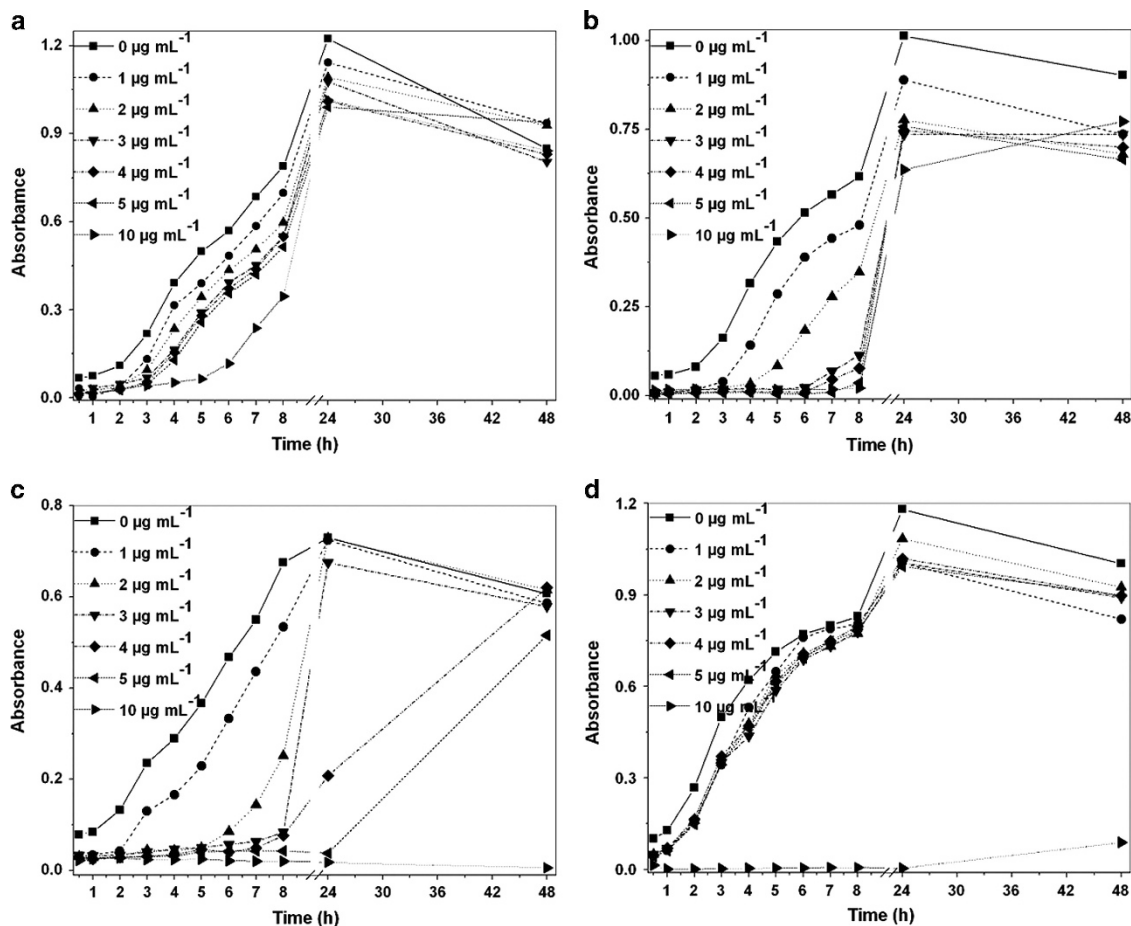


**Figure 1** The growth curve of bacteria in nutrient broth supplemented with different concentrations (1–10  $\mu\text{g mL}^{-1}$ ) of silver nanoparticles synthesized with gum ghatti (Ag NP-GT), (a) *E. coli* 25922, (b) *E. coli* 35218, (c) *P. aeruginosa* 27853 and (d) *S. aureus* 25923.

the lower concentrations up to  $4 \mu\text{g mL}^{-1}$  inhibited the growth for 5 h only. The growth was resumed with  $10 \mu\text{g mL}^{-1}$  of nanoparticles, after 24 h (Figure 2a). But with 10–15-nm-sized silver nanoparticles, even a higher concentration of  $25 \mu\text{g mL}^{-1}$  limited the lag phase to about 8 h only for *E. coli* 25922.<sup>29</sup>

In the case of the Gram-negative *E. coli* 35218 strain, the concentrations of 1 and  $2 \mu\text{g mL}^{-1}$  of Ag NP-GT did not cause inhibition. Although the concentrations of 3– $10 \mu\text{g mL}^{-1}$  induced a lag phase for 8 h, beyond 24 h the cells survived the nanoparticle stress and the growth continued (Figure 1b). In the case of Ag NP-OB, the concentrations beyond  $1 \mu\text{g mL}^{-1}$  induced the lag phase for 8 h and the growth was resumed after 8 and 24 h of incubation with 2–3 and 4– $5 \mu\text{g mL}^{-1}$  of nanoparticles, respectively. At a concentration of  $10 \mu\text{g mL}^{-1}$ , the growth was completely inhibited (Figure 2b). In an earlier antibacterial characterization study carried out with silver nanoparticles of 16 nm size against another *E. coli* strain ATCC 15224, no bacterial growth was noted at  $60 \mu\text{g mL}^{-1}$  concentration.<sup>30</sup> But such phenomenon of complete inhibition was observed at  $10 \mu\text{g mL}^{-1}$  concentration itself with Ag NP-OB against *E. coli* 35218. With the same strain of *E. coli* 35218 and polylysine-capped silver nanoparticles of 7.2 nm size, a concentration of  $50 \mu\text{g mL}^{-1}$  only extended the lag phase for 5 h.<sup>31</sup> For the *P. aeruginosa* 27853, the lag phase was lengthened by 8 and 24 h with 3–4 and 5– $10 \mu\text{g mL}^{-1}$  of Ag NP-GT, respectively. At a concentration of  $10 \mu\text{g mL}^{-1}$ , the growth was arrested completely (Figure 1c). With Ag NP-OB, the lag phase was

expanded by 8 and 24 h with 3 and 4– $10 \mu\text{g mL}^{-1}$ , respectively, and  $10 \mu\text{g mL}^{-1}$  of nanoparticles totally seized the growth (Figure 2c). Thus, all the Gram-negative strains showed similar trend of growth inhibition (Ag NP-OB > Ag NP-GT) with the nanoparticles tested.

Nevertheless, with Ag NP-GT and Ag NP-OB, a concentration of  $10 \mu\text{g mL}^{-1}$  was able to stop the cell division totally for the Gram-positive *S. aureus* 25923 and the concentrations below  $10 \mu\text{g mL}^{-1}$  did not induce lag phase (Figures 1d and 2d). The order of inhibition was found to be Ag NP-OB  $\geq$  Ag NP-GT for *S. aureus* 25923. With the same strain of *S. aureus* 25923, the concentration of  $100 \mu\text{g mL}^{-1}$  elicited only a partial growth inhibition with silver nanoparticles 10–15 nm synthesized with glucose and hydrazine.<sup>29</sup> The bacterial cultures without nanoparticles did not show any inhibition and reached the stationary phase at the end of 48 h. The enhanced growth inhibition activity of the biogenic nanoparticles can be attributed to superior stability of the nanoparticle solutions.<sup>29</sup> The data on growth curve indicates a faster inhibition in Gram-negative bacteria compared with Gram-positive bacteria.<sup>21,29</sup> Thus, the inhibition of growth depends on the type of bacterial strain as well as the concentration and particle size of nanoparticles.

#### Leakage of cytoplasmic contents

The damage to bacterial cytoplasmic membrane induced by silver nanoparticles was studied in terms of leakage of cytoplasmic contents.<sup>19</sup> The amount of nucleic acids and proteins released into



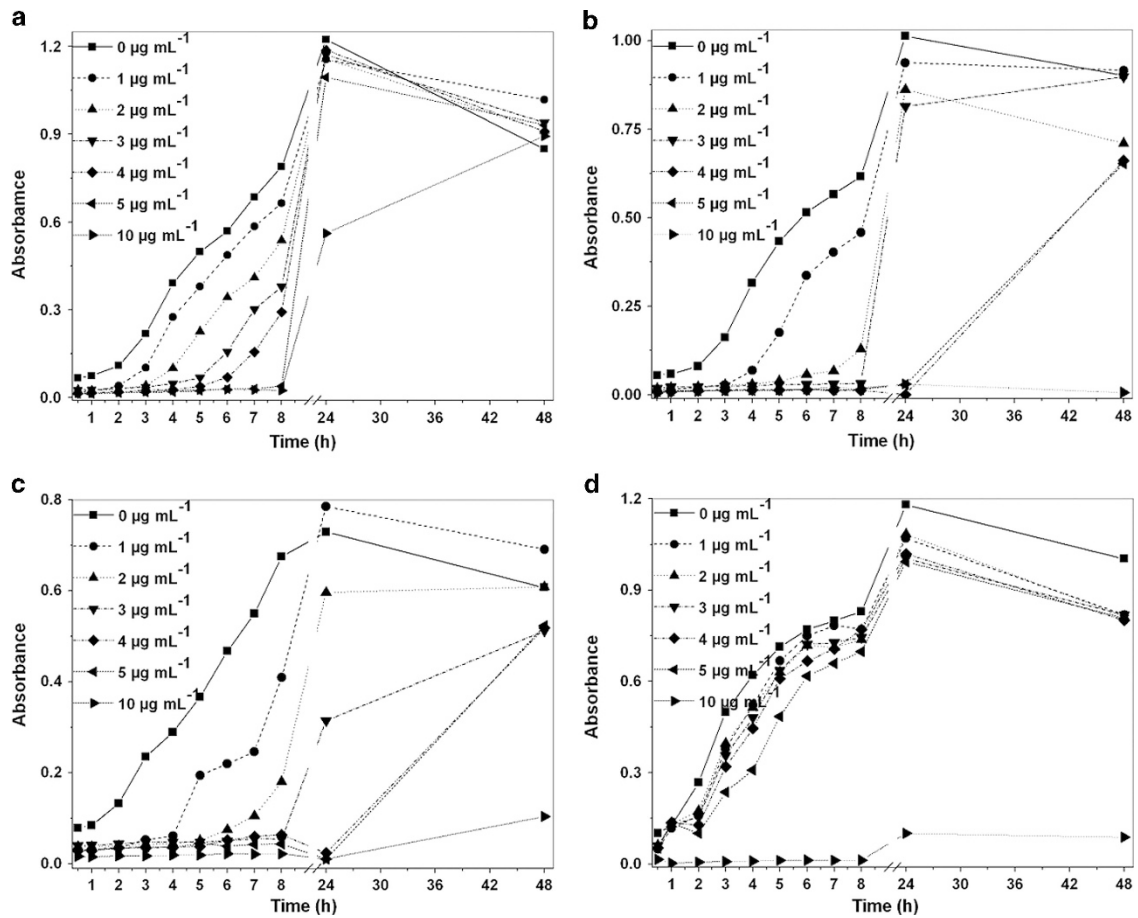


**Figure 2** The growth curve of bacteria in nutrient broth supplemented with different concentrations (1–10  $\mu\text{g ml}^{-1}$ ) of silver nanoparticles synthesized with gum olibanum (Ag NP-OB), (a) *E. coli* 25922, (b) *E. coli* 35218, (c) *P. aeruginosa* 27853 and (d) *S. aureus* 25923.

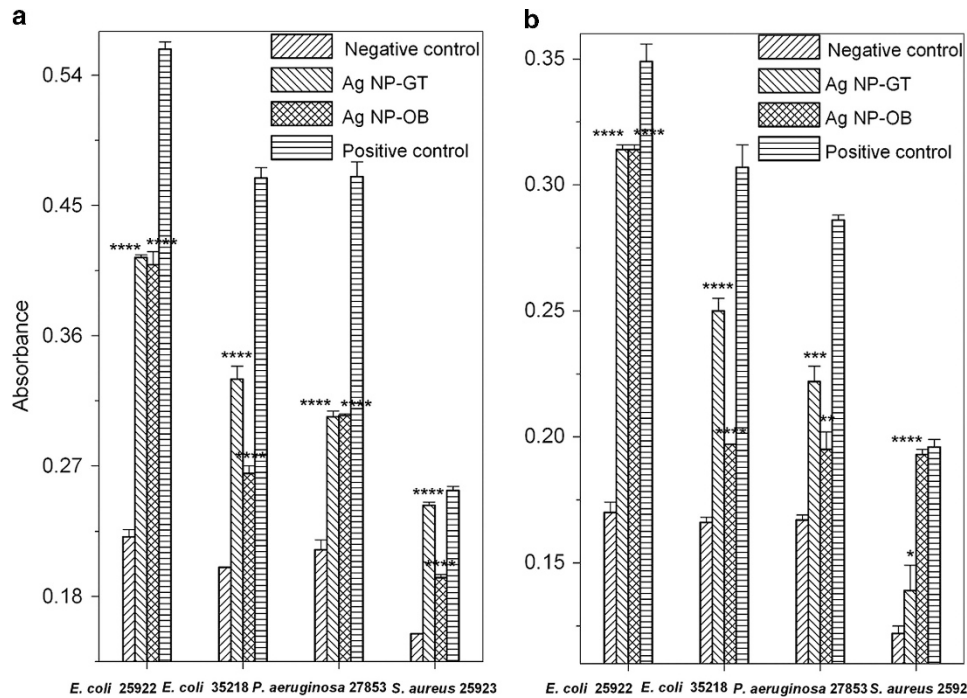


**Figure 3** The release of (a) 260-nm and (b) 280-nm absorbing materials from the cell suspensions of bacteria treated with silver nanoparticles (Ag NP)-synthesized with gum ghatti (GT) and Ag NP-synthesized with gum olibanum (OB). Values are mean  $\pm$  s.d. ( $n=3$ ); \* $P<0.05$ , \*\* $P<0.005$ , \*\*\* $P<0.001$  and \*\*\*\* $P<0.0001$  compared with negative control.

the suspension was determined by measuring the absorbance at 260 and 280 nm. At  $5 \mu\text{g ml}^{-1}$  concentration of nanoparticles, the highest release of nucleic acids and proteins was observed with *E. coli* 25922, followed by *E. coli* 35218, *P. aeruginosa* 27853 and *S. aureus* 25923. The release of nucleic acids were found to be in the order Ag NP-GT > Ag NP-OB for the *E. coli* 25922, *E. coli* 35218 and *S. aureus* 25923; and Ag NP-OB  $\geq$  Ag NP-GT for *P. aeruginosa* 27853. In the case protein leakage, the order was Ag NP-GT > Ag NP-OB for *E. coli* 35218 and *P. aeruginosa* 27853; Ag NP-GT = Ag NP-OB for *E. coli* 25922 and Ag NP-OB > Ag NP-GT for *S. aureus* 25923, respectively (Figure 3). Among the selected strains, the strain *S. aureus* 25923 was more resistant to nanoparticles when compared with other Gram-negative strains.<sup>21</sup>

#### Outer membrane damage

The outer membrane permeabilization activity of biogenic nanoparticles was assessed by measuring the characteristic fluorescence via uptake of hydrophobic NPN. It is mainly due to the destabilizing

interaction of nanoparticles with membrane components.<sup>22</sup> At  $3 \mu\text{g ml}^{-1}$  concentration of nanoparticles, the outer membrane damage was Ag NP-GT > Ag NP-OB for all the Gram-negative bacterial strains (Figure 4). From the data, it is apparent that among the Gram-negative strains, *E. coli* 35218 was least susceptible to the outer membrane permeabilization by both the nanoparticles. Interestingly, in *E. coli* 35218 the activity of the both the nanoparticle preparations was more than the positive control hydrogen peroxide.

#### Effect of antioxidant on the bactericidal activity of silver nanoparticles

The involvement of ROS in the antibacterial effect of silver nanoparticles was studied using NAC as an antioxidant. In the control petri plates with NAC alone, the bacterial colonies were clearly seen with no growth inhibition. However, in the petri plates supplemented with  $5 \mu\text{g ml}^{-1}$  of Ag NP-GT nanoparticles, no bacterial colonies were observed due to complete inhibition of growth. Whereas in the petri plates supplemented with both NAC and silver nanoparticles the

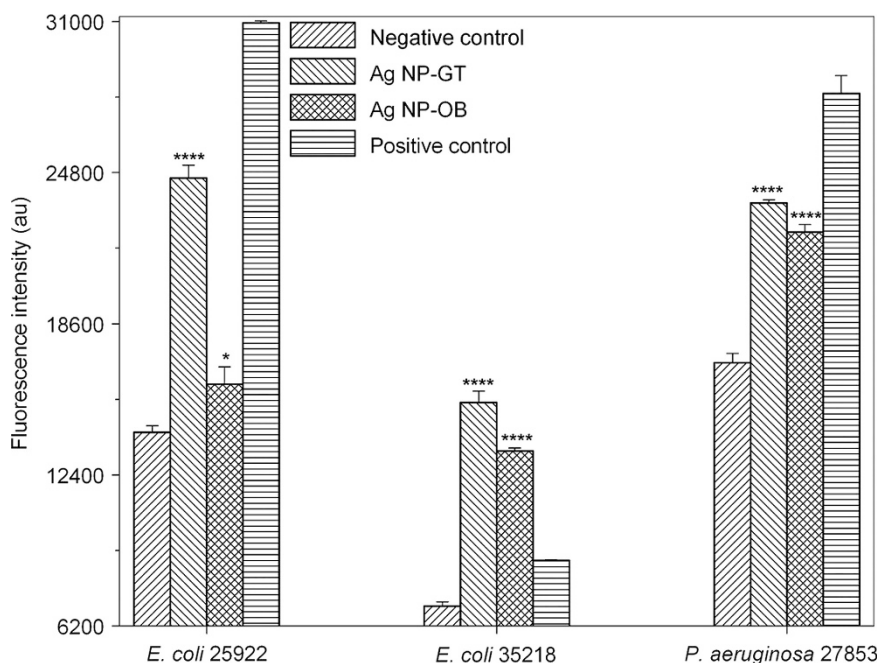


**Figure 4** The uptake of *N*-phenyl naphthylamine (NPN) in bacteria induced by treatment with silver nanoparticles (Ag NP)-synthesized with gum ghatti (GT) and Ag NP-synthesized with gum olibanum (OB). Values are mean  $\pm$  s.d. ( $n=3$ ); \* $P<0.05$  and \*\*\*\* $P<0.0001$  compared with negative control.

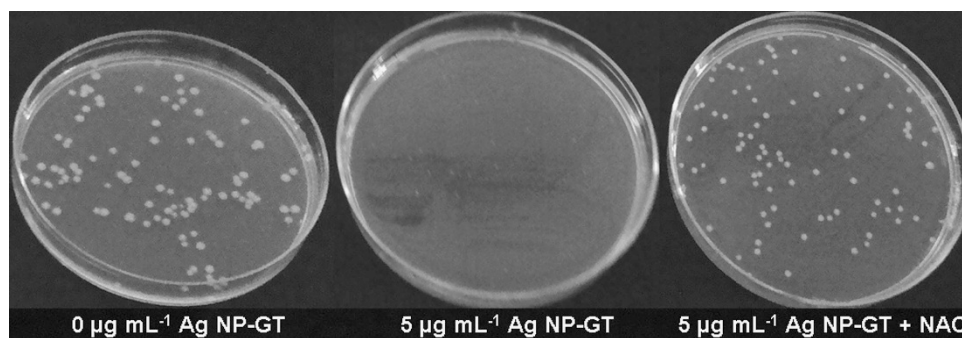


**Figure 5** The Petri plates showing the effect of antioxidant *N*-acetylcysteine (NAC) on the bactericidal activity of silver nanoparticles synthesized with gum ghatti (Ag NP-GT) on *E. coli* 35218. A full color version of this figure is available at *The Journal of Antibiotics* journal online.

bacterial colonies were observed (Figure 5). From these photographs, it is evident that ROS are involved in the bactericidal activity of nanoparticles, and NAC acted as a scavenger and protected the *E. coli* 35218 cells from Ag NP-GT. This observation is in concurrence with earlier studies on antimicrobial effects of silver nanoparticles.<sup>12</sup>

The percentage survival of bacteria in the presence of NAC and silver nanoparticles is depicted in Figure 6. For the Gram-positive *S. aureus*, NAC was able to protect the bacterial cells almost completely (97% and 93.4%) from the toxicity of Ag NP-GT and Ag NP-OB, respectively. A similar trend was observed with other Gram-negative

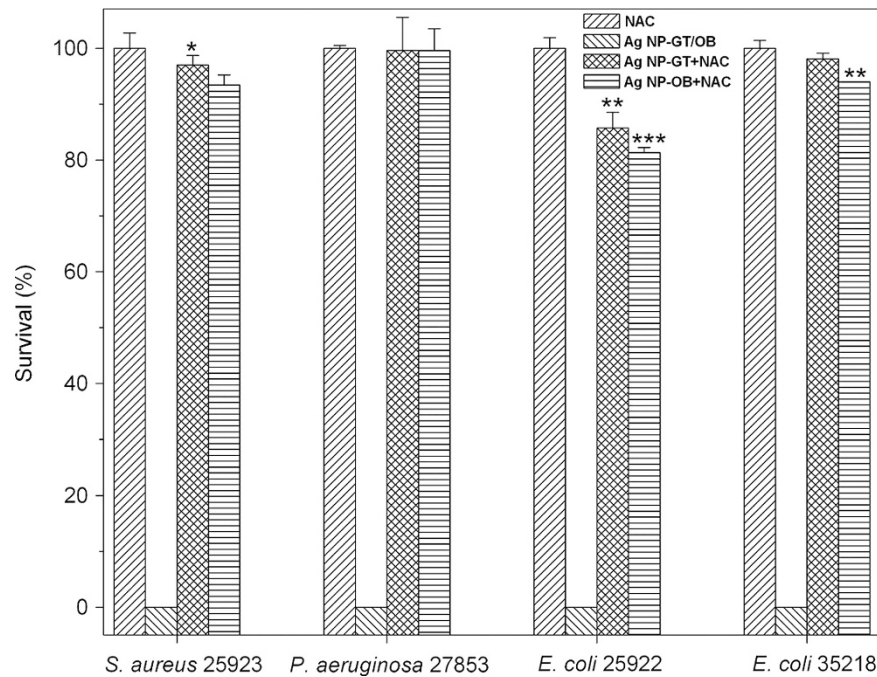


**Figure 6** The bar graph showing the percentage of viable cells in the presence of antioxidant *N*-acetylcysteine (NAC) and  $5\mu\text{g ml}^{-1}$  of silver nanoparticles (Ag NP)-synthesized with gum ghatti (GT) and Ag NP-synthesized with gum olibanum (OB). Values are mean  $\pm$  s.d. ( $n=3$ ); \* $P<0.05$ , \*\* $P<0.005$  and \*\*\* $P<0.001$  compared with control.

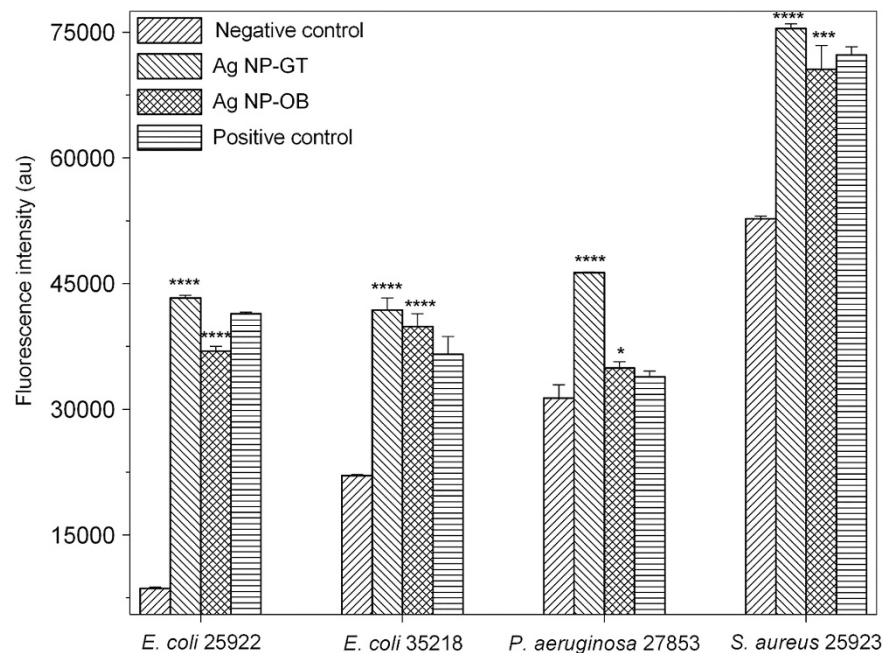


**Figure 7** The production of intracellular ROS in the bacterial cell suspensions treated with silver nanoparticles (Ag NP)-synthesized with gum ghatti (GT) and Ag NP-synthesized with gum olibanum (OB). Values are mean  $\pm$  s.d. ( $n=3$ ); \* $P<0.05$  and \*\*\*\* $P<0.0001$  compared with negative control.



strains *P. aeruginosa* 27853 (99.6%) and *E. coli* 35218 (98.1% and 94%), respectively. However, NAC was able to protect only 85.7% and 81.3% of cells from Ag NP-GT and Ag NP-OB, respectively, for *E. coli*

25922. Among the selected strains, *E. coli* 25922 was found to be more sensitive and was unable to recover completely from the bactericidal activity of nanoparticles, even with NAC supplementation.

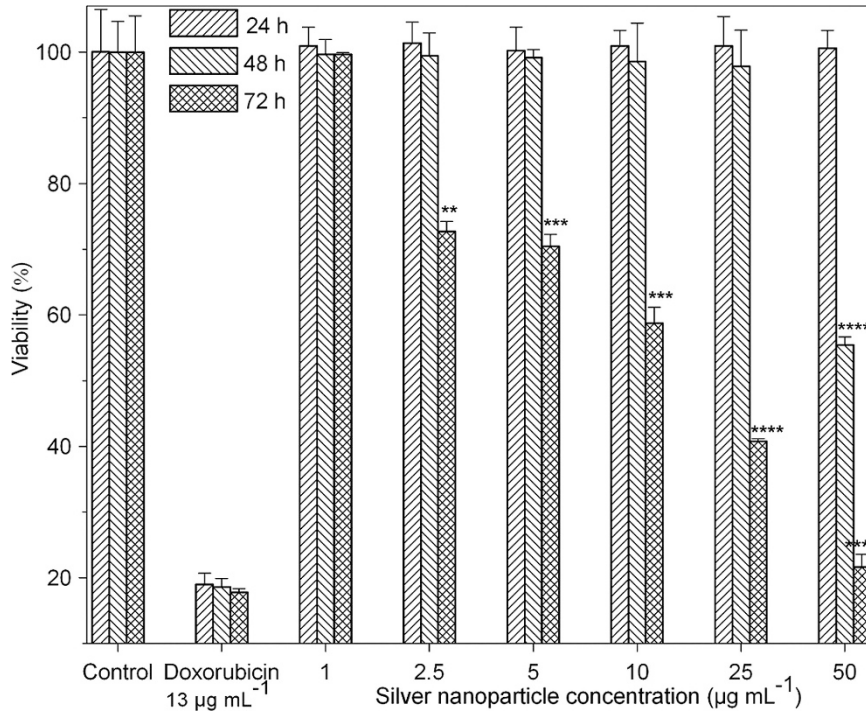


**Figure 8** The effect of silver nanoparticles synthesized with gum ghatti (Ag NP-GT) on the cell viability of HeLa cell line at various concentrations. Values are mean  $\pm$  s.d. ( $n=3$ ); \*\* $P<0.005$ , \*\*\* $P<0.001$  and \*\*\*\* $P<0.0001$  compared with untreated cells.

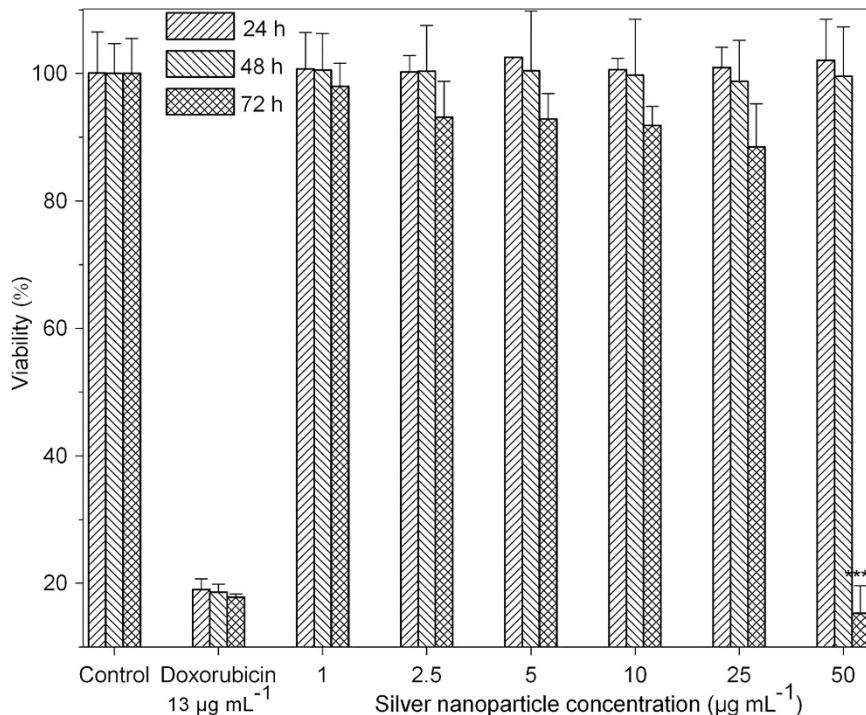


**Figure 9** The effect of silver nanoparticles synthesized with gum olibanum (Ag NP-OB) on the cell viability of HeLa cell line at various concentrations. Values are mean  $\pm$  s.d. ( $n=3$ ); \*\*\*\* $P<0.0001$  compared with untreated cells.



### Detection of intracellular ROS

The response of bacterial strains toward biogenic nanoparticles is depicted in terms of ROS production, an indicator for cellular oxidative stress. For *S. aureus* 25923, *E. coli* 25922 and *E. coli* 35218, the generation of ROS is comparable with positive control 30  $\mu\text{M}$   $\text{H}_2\text{O}_2$ , at 2  $\mu\text{g ml}^{-1}$  of silver nanoparticles. In the case of *P. aeruginosa* 27853, the intracellular ROS was more than the positive control (Figure 7). Among the selected strains, the production of intracellular ROS was highest in *S. aureus* 25923. From the graph, it is evident that the generation of intracellular ROS was found to be Ag NP-GT > Ag NP-OB for all the tested strains.

### Cytotoxicity evaluation

The biocompatibility of the biogenic silver nanoparticles with HeLa cell line was evaluated in terms of cell proliferation. The percentage viability of the cells was plotted against various nanoparticle concentrations at different time intervals. With Ag NP-GT, the nanoparticles were biocompatible only at 1  $\mu\text{g ml}^{-1}$  concentration. From 2.5  $\mu\text{g ml}^{-1}$  onward they were cytotoxic and the viability was reduced to 70.4%, 58.7%, 40.7% and 21.6% at the respective concentrations of 5, 10, 25 and 50  $\mu\text{g ml}^{-1}$  at 72 h (Figure 8). Hence,

**Table 3 Comparative account of the antibacterial activity of Ag NP-GT and Ag NP-OB**

| Test parameter                | Efficacy                 | Applicable strains         |
|-------------------------------|--------------------------|----------------------------|
| ZOI                           | Ag NP-GT > Ag NP-OB      | All test strains           |
| <i>Antibacterial activity</i> |                          |                            |
| MIC                           | Ag NP-GT = Ag NP-OB      | All test strains           |
| MBC                           | Ag NP-GT = Ag NP-OB      | <i>E. coli</i> 25922       |
|                               | Ag NP-GT > Ag NP-OB      | <i>P. aeruginosa</i> 27853 |
|                               |                          | <i>E. coli</i> 35218       |
|                               |                          | <i>S. aureus</i> 25923     |
| Growth inhibition             | Ag NP-OB > Ag NP-GT      | <i>E. coli</i> 25922       |
|                               | Ag NP-OB $\geq$ Ag NP-GT | <i>E. coli</i> 35218       |
|                               |                          | <i>P. aeruginosa</i> 27853 |
|                               |                          | <i>S. aureus</i> 25923     |
| Antibiofilm activity          | Ag NP-GT = Ag NP-OB      | All test strains           |
| Leakage of nucleic acids      | Ag NP-GT > Ag NP-OB      | <i>E. coli</i> 25922       |
|                               | Ag NP-OB $\geq$ Ag NP-GT | <i>E. coli</i> 35218       |
|                               |                          | <i>S. aureus</i> 25923     |
|                               |                          | <i>P. aeruginosa</i> 27853 |
| Leakage of proteins           | Ag NP-GT > Ag NP-OB      | <i>E. coli</i> 35218       |
|                               | Ag NP-GT = Ag NP-OB      | <i>P. aeruginosa</i> 27853 |
|                               | Ag NP-OB > Ag NP-GT      | <i>E. coli</i> 25922       |
|                               |                          | <i>S. aureus</i> 25923     |
| Outer membrane damage         | Ag NP-GT > Ag NP-OB      | <i>E. coli</i> 25922       |
|                               |                          | <i>E. coli</i> 35218       |
|                               |                          | <i>P. aeruginosa</i> 27853 |
| ROS and bactericidal activity | Ag NP-OB $\geq$ Ag NP-GT | <i>E. coli</i> 35218       |
|                               |                          | <i>E. coli</i> 25922       |
|                               |                          | <i>S. aureus</i> 25923     |
|                               |                          | <i>P. aeruginosa</i> 27853 |
| Intracellular ROS production  | Ag NP-GT > Ag NP-OB      | All test strains           |
| <i>Biocompatibility</i>       |                          |                            |
| Cytotoxicity                  | Ag NP-GT > Ag NP-OB      | HeLa cell line             |

Abbreviations: Ag NP-GT, silver nanoparticles synthesized with gum ghatti; Ag NP-OB, silver nanoparticles synthesized with gum olibanum; ROS, reactive oxygen species; ZOI, zone of inhibition.

the Ag NP-GT elicited a dose-dependent effect on the proliferation of HeLa cell line in MTT assay.<sup>32,33</sup> Whereas with Ag NP-OB, the cytotoxic effect was observed only at 50  $\mu\text{g ml}^{-1}$  (15.2%) and the concentrations up to 25  $\mu\text{g ml}^{-1}$  were not cytotoxic (Figure 9). The biogenic nanoparticles of 5.7 nm size (Ag NP-GT) were cytotoxic beyond 2.5  $\mu\text{g ml}^{-1}$ , whereas with 7.5 nm size (Ag NP-OB) they were biocompatible up to a concentration of 25  $\mu\text{g ml}^{-1}$ . With latex-capped silver nanoparticles of 10 nm size, the antiproliferation effect was noted at 100  $\mu\text{g ml}^{-1}$ .<sup>32</sup> Thus, the results indicate a dependency of cytotoxic concentration on particle size. These results are in tune with earlier cytotoxic studies carried out with chitosan nanoparticles of different sizes. Also, the enhanced cytotoxicity of the Ag NP-GT can be correlated to its higher zeta potential values in comparison with Ag NP-OB.<sup>33</sup> On the basis of these observations, it can be concluded that the synthesized biogenic nanoparticles have dual potential applications.<sup>16</sup> The nanoparticles with superior toxicity (Ag NP-GT) may be employed as cytotoxic bactericidal agents, whereas the benign ones (Ag NP-OB) as biocompatible bactericidal agents.

The antibacterial activity of both the biogenic silver nanoparticles was compared in terms of ZOI, MIC, MBC, inhibition of growth kinetics, antibiofilm activity, membrane damage, ROS production and cytotoxicity (Table 3). It was observed that with most of the used parameters, the efficacy of Ag NP-GT was more than Ag NP-OB. The enhanced antibacterial and cytotoxicity activities of Ag NP-GT could be attributed to the smaller size, monodispersity and zeta potential of the nanoparticles (Table 4). The gum ghatti is an arabinogalactan type of gum and is composed of sugars such as arabinose, galactose, mannose, xylose, rhamnose and glucuronic acid. It has a MW of  $8.9 \times 10^7 \text{ g mol}^{-1}$ , protein rich and the protein content was reported to be in the range of 2.8–3.7%.<sup>9</sup> The gum olibanum is categorized under glucuronoarabinogalactan type and is composed of arabinose, galactose, xylose and glucuronic acid. It has a MW of  $5.1\text{--}5.6 \times 10^5 \text{ g mol}^{-1}$  and the protein content was reported to be 3.4%.<sup>10</sup> Although both the nanoparticles are protein capped, they differ in protein content and composition of the gum, which leads to a difference in the surface functionalization of nanoparticles and zeta potential values.

**Table 4 Comparative account of the physical properties of Ag NP-GT and Ag NP-OB**

| Parameter                         | Ag NP-GT <sup>9</sup>   | Ag NP-OB <sup>10</sup>                           |
|-----------------------------------|---|--|
| Gum used                          | Gum ghatti  | Gum olibanum                                     |
| Type of gum                       | Arabinogalactan   | Glucuronoarabinogalactan                         |
| Gum composition                   | Arabinose, galactose, mannose, xylose, rhamnose and glucuronic acid | Arabinose, galactose, xylose and glucuronic acid |
| MW of gum ( $\text{g mol}^{-1}$ ) | $8.9 \times 10^7$   | $5.1\text{--}5.6 \times 10^5$                    |
| Protein content in gum (%)        | 2.8–3.7   | 3.4  |
| Particle range (nm)               | 4.8–6.2   | 1.9–14.7   |
| Average particle size (nm)        | $5.7 \pm 0.2$   | $7.5 \pm 3.8$                                    |
| Monodispersed particles (%)       | 70  | 50   |
| Zeta potential (mV)               | $-22.4 \pm 8.7$   | $-14.9 \pm 6.6$                                  |

Abbreviations: Ag NP-GT, silver nanoparticles synthesized with gum ghatti; Ag NP-OB, silver nanoparticles synthesized with gum olibanum.

## CONCLUSIONS

The highly stable biogenic silver nanoparticles had significant antibacterial action on planktonic and biofilm modes of bacterial growth against Gram-negative and Gram-positive bacteria. Also, the ZOI, MIC and MBC values observed are higher than the reported values. Thus, the biogenic antibacterial silver nanoparticles generated with gums have an advantage over the other chemogenic silver nanoparticles. Among the selected strains, Gram-positive *S. aureus* 25923 was more resistant to membrane damage and growth curve inhibition when compared with other Gram-negative strains tested. The biocompatibility of the silver nanoparticles with HeLa indicated the dependency of cytotoxic concentration on particle size and zeta potential. It was found that Ag NP-GT was a more potent bactericidal and cytotoxic agent than Ag NP-OB. The enhanced antibacterial activity of Ag NP-GT enables it to be an effective bactericidal agent, whereas the non-cytotoxic nature of Ag NP-OB makes it a candidate of choice for biocompatible bactericidal activity. Further studies need to be carried out to find out the actual surface functional molecules that are responsible for differential activity of these biogenic silver nanoparticles capped with proteins from natural plant gums.

## ACKNOWLEDGEMENTS

We thank Dr J. Arunachalam, Former Head, NCCCM for his constant support and encouragement.

- 1 Raveendran, P., Fu, J. & Wallen, S. L. Completely 'green' synthesis and stabilization of metal nanoparticles. *J. Am. Chem. Soc.* **125**, 13940–13941 (2003).
- 2 Vigneshwaran, N., Nachane, R. P., Balasubramanya, R. H. & Varadarajan, P. V. A novel one-pot 'green' synthesis of stable silver nanoparticles using soluble starch. *Carbohydr. Res.* **341**, 2012–2018 (2006).
- 3 Gericke, M. & Pinches, A. Microbial production of gold nanoparticles. *Gold Bull.* **39**, 22–28 (2006).
- 4 Kumar, C. G. & Mamidyala, S. K. Extracellular synthesis of silver nanoparticles using culture supernatant of *Pseudomonas aeruginosa*. *Colloid. Surf. B* **84**, 462–466 (2011).
- 5 Vigneshwaran, N. *et al.* Biological synthesis of silver nanoparticles using the fungus *Aspergillus flavus*. *Mater. Lett.* **61**, 1413–1418 (2007).
- 6 Govindaraju, K., Kiruthiga, V., Kumar, V. G. & Singaravelu, G. Extracellular synthesis of silver nanoparticles by a marine alga, *Sargassum wightii* Grevilli and their antibacterial effects. *J. Nanosci. Nanotechnol.* **9**, 5497–5501 (2009).
- 7 Shankar, S. S., Rai, A., Ahmad, A. & Sastry, M. Rapid synthesis of Au, Ag, and bimetallic Au core-Ag shell nanoparticles using neem (*Azadirachta indica*) leaf broth. *J. Colloid Interf. Sci.* **275**, 496–502 (2004).
- 8 Thakkar, K. N., Mhatre, S. S. & Parikh, R. Y. Biological synthesis of metallic nanoparticles. *Nanomed. Nanotechnol. Biol. Med.* **6**, 257–262 (2010).
- 9 Kora, A. J., Sashidhar Rao, B. & Jayaraman, A. Size-controlled green synthesis of silver nanoparticles mediated by gum ghatti (*Anogeissus latifolia*) and its biological activity. *Org. Med. Chem. Lett.* **2**, 1–10 (2012).
- 10 Kora, A. J., Sashidhar, R. B. & Arunachalam, J. Aqueous extract of gum olibanum (*Boswellia serrata*): a reductant and stabilizer for the biosynthesis of antibacterial silver nanoparticles. *Process Biochem.* **47**, 1516–1520 (2012).
- 11 Cho, K.-H., Park, J.-E., Osaka, T. & Park, S.-G. The study of antimicrobial activity and preservative effects of nanosilver ingredient. *Electrochim. Acta* **51**, 956–960 (2005).
- 12 Kim, J. S. *et al.* Antimicrobial effects of silver nanoparticles. *Nanomed. Nanotechnol. Biol. Med.* **3**, 95–101 (2007).
- 13 Panacek, A. *et al.* Silver colloid nanoparticles: synthesis, characterization, and their antibacterial activity. *J. Phys. Chem. B* **110**, 16248–16253 (2006).
- 14 Sharma, V. K., Yngard, R. A. & Lin, Y. Silver nanoparticles: green synthesis and their antimicrobial activities. *Adv. Colloid Interf. Sci.* **145**, 83–96 (2009).
- 15 Sondi, I. & Salopek-Sondi, B. Silver nanoparticles as antimicrobial agent: a case study on *E. coli* as a model for Gram-negative bacteria. *J. Colloid Interf. Sci.* **275**, 177–182 (2004).
- 16 Suresh, A. K. *et al.* Silver nanocrystallites: Biofabrication using *Shewanella oneidensis*, and an evaluation of their comparative toxicity on Gram-negative and Gram-positive bacteria. *Environ. Sci. Technol.* **44**, 5210–5215 (2010).
- 17 Martinez-Castanon, G. A., Nino-Martinez, N., Martinez-Gutierrez, F., Martinez-Mendoza, J. R. & Ruiz, F. Synthesis and antibacterial activity of silver nanoparticles with different sizes. *J. Nanopart. Res.* **10**, 1343–1348 (2008).
- 18 Uhlich, G. A., Cooke, P. H., & Solomon, E. B. Analyses of the red-dry-rough phenotype of an *Escherichia coli* O157:H7 strain and its role in biofilm formation and resistance to antibacterial agents. *Appl. Environ. Microbiol.* **72**, 2564–2572 (2006).
- 19 Chen, C. Z. & Cooper, S. L. Interactions between dendrimer biocides and bacterial membranes. *Biomaterials* **23**, 3359–3368 (2002).
- 20 Liu, H., Du, Y., Wang, X. & Sun, L. Chitosan kills bacteria through cell membrane damage. *Inter. J. Food Microbiol.* **95**, 147–155 (2004).
- 21 Tiwari, D. K., Behari, J. & Sen, P. Time and dose-dependent antimicrobial potential of Ag nanoparticles synthesized by top-down approach. *Curr. Sci.* **95**, 647–655 (2008).
- 22 Helander, I. M. & Mattila-Sandholm, T. Fluorometric assessment of Gram-negative bacterial permeabilization. *J. Appl. Microbiol.* **88**, 213–219 (2000).
- 23 Ahamed, M., Majeed Khan, M. A., Siddiqui, M. K. J., AlSalhi, M. S. & Alrokayan, S. A. Green synthesis, characterization and evaluation of biocompatibility of silver nanoparticles. *Physica E* **43**, 1266–1271 (2011).
- 24 Du, W.-L., Niu, S.-S., Xu, Y.-L., Xu, Z.-R. & Fan, C.-L. Antibacterial activity of chitosan tripolyphosphate nanoparticles loaded with various metal ions. *Carbohydr. Polym.* **75**, 385–389 (2009).
- 25 Ruparelia, J. P., Chatterjee, A. K., Duttgupta, S. P. & Mukherji, S. Strain specificity in antimicrobial activity of silver and copper nanoparticles. *Acta Biomater.* **4**, 707–716 (2008).
- 26 Jaidev, L. R. & Narasimha, G. Fungal mediated biosynthesis of silver nanoparticles, characterization and antimicrobial activity. *Colloid. Surf. B* **81**, 430–433 (2010).
- 27 Kora, A. J., Manjusha, R. & Arunachalam, J. Superior bactericidal activity of SDS capped silver nanoparticles: Synthesis and characterization. *Mater. Sci. Eng. C* **29**, 2104–2109 (2009).
- 28 Mohanty, S. *et al.* An investigation on the antibacterial, cytotoxic, and antibiofilm efficacy of starch-stabilized silver nanoparticles. *Nanomed. Nanotechnol. Biol. Med.* **8**, 916–924 (2012).
- 29 Siddhartha, S. *et al.* Characterization of enhanced antibacterial effects of novel silver nanoparticles. *Nanotechnology* **18**, 225103–225111 (2007).
- 30 Raffi, M. *et al.* Antibacterial characterization of silver nanoparticles against *E. Coli* ATCC-15224. *J. Mater. Sci. Technol.* **24**, 192–196 (2008).
- 31 Dror-Ehre, A., Mamane, H., Belenkova, T., Markovich, G. & Adin, A. Silver nanoparticle-*E. coli* colloidal interaction in water and effect on *E. coli* survival. *J. Colloid Interf. Sci.* **339**, 521–526 (2009).
- 32 Valodkar, M. N., Jadeja, R. C., Thounaojam, M. V., Devkar, R. & Thakore, S. *In vitro* toxicity study of plant latex capped silver nanoparticles in human lung carcinoma cells. *Mater. Sci. Eng. C* **31**, 1723–1728 (2011).
- 33 Qi, L., Xu, Z., Jiang, X., Li, Y. & Wang, M. Cytotoxic activities of chitosan nanoparticles and copper-loaded nanoparticles. *Bioorg. Med. Chem. Lett.* **15**, 1397–1399 (2005).

Supplementary Information accompanies the paper on The Journal of Antibiotics website (<http://www.nature.com/ja>)